Renewable Energy xxx (xxxx) xxx

Contents lists available at ScienceDirect

Renewable Energy

journal homepage: www.elsevier.com/locate/renene

Stabilization of K_2CO_3 in vermiculite for thermochemical energy storage

A.I. Shkatulov [a], J. Houben [a], H. Fischer [b], H.P. Huinink [a, *]

[a] Eindhoven University of Technology, Department of Applied Physics, De Rondom 70, 5612 AP, Eindhoven, the Netherlands
[b] TNO, High Tech Campus 25, 5656 AE, Eindhoven, the Netherlands

ARTICLE INFO

Article history:
Received 29 August 2019
Received in revised form
13 November 2019
Accepted 23 November 2019
Available online xxx

Keywords:
Thermochemical energy storage
Sorption heat storage
Potassium carbonate
Salt hydrates
Composites
Vermiculite

ABSTRACT

Thermochemical energy storage (TCES) is an emerging technology promising for domestic applications. Recently, K_2CO_3 was identified and studied as a TCES material. In this work, the composite "K_2CO_3 in expanded vermiculite" (69 wt. % of the salt) was prepared and studied for thermochemical energy storage bearing in mind its application for space heating. The hydration rate was found to be higher for the confined K_2CO_3 in comparison with K_2CO_3 granules of the same size. While morphology and texture of the composite alter after 74 hydration/dehydration cycles, its chemical composition and average grain size do not change. The energy storage density of the composite bed can reach 0.9 GJ/m^3 (250 kWh/m^3) for cycles with deliquescence which makes the composite an inexpensive thermochemical material for space heating. Stable conversion for deliquescence conditions was shown for at least 47 cycles.

1. Introduction

Widespread use of renewable energies and implementation of energy efficiency policies are currently considered as cornerstones of future energy systems [1]. Nowadays around 70% of all the energy consumed by the residential sector in the European Union is used for space heating while around 10% is used to heat up water [2]. Direct use of solar energy for these purposes is complicated by decoupling heat supply and heat demand. This difficulty makes storage of thermal energy a crucial task in implementation of renewable and sustainable energy systems and spurs development of thermal energy storage systems.

The existing approaches to thermal energy storage harnessing sensible or latent heat of materials are generally acknowledged as technologically mature [3]. A promising alternative to these technologies is thermochemical energy storage (TCES) involving reversible chemical reactions for storage of heat in a form of chemical species. TCES provides high heat storage density (> 1 GJ/m^3) due to the high heat effects of chemical reactions and theoretically infinite storage time due to separate storage of reagents and products [4].

Among many chemical transformations considered for TCES, the dehydration/hydration reactions have been in the spotlight since the late 1970s [5] as the water is easy-to-handle and environmentally benign working fluid. The dehydration-hydration of salt hydrates have started attracting increasing researchers' attention during the last decade which resulted in several studies dedicated to the systematic screening of the salt hydrates for TCES aimed at expanding the "shortlist" of candidate salts [6–10].

One of such studies by Donkers et al. [8] surveys 563 salt hydrates, bearing in mind their potential application in a TCES system which must be charged by solar or waste heat (100 °C) in order to be able to upgrade heat from 10 °C (underground water) to 40–60 °C (useful heat) at the discharging stage (Fig. 1). In that study, potassium carbonate, K_2CO_3, was identified as one of the salts that meets thermodynamic criteria for the boundary conditions of the thermochemical cycle [11]. This salt forms a sesquihydrate ($K_2CO_3 \cdot 1.5H_2O$) that can be dehydrated to store heat:

$$K_2CO_3 \cdot 1.5H_2O_{(s)} = K_2CO_{3\,(s)} + 1.5\,H_2O_{\,(g)}\ \Delta_r H^o_{298} = 98\ \text{kJ/mol}\ [12] \quad (1)$$

The heat stored in the form of the anhydrous salt may be released on demand by hydration of K_2CO_3 with water vapor (the reverse reaction (1)). Unlike many other salts proposed in the literature, potassium carbonate is inexpensive, corrosion inactive

* Corresponding author.
E-mail address: h.p.huinink@tue.nl (H.P. Huinink).

https://doi.org/10.1016/j.renene.2019.11.119

Nomenclature

Abbreviations

DVS	Dynamic Vapor Sorption
EDS	Energy Dispersive Spectroscopy
MIP	Mercury Intrusion Porosimetry
PCM	Phase-change material
SEM	Scanning Electron Microscopy
TG	Thermogravimetric
TGA	Thermogravimetric Analysis
TCES	Thermochemical Energy Storage
VSD_{ab}	Volumetric Storage Density with absorption, GJ/m^3
VSD_r	Volumetric Storage Density with reaction only, GJ/m^3
$VSD_{K_2CO_3}$	Volumetric Storage Density of pure K_2CO_3, GJ/m^3
XRD	X-Ray Diffraction

Latin symbols

a	equilibrium water uptake, (g-H_2O)/(g-K_2CO_3/V)
a_0	equilibrium water uptake after formation of $K_2CO_3 \cdot 1.5H_2O$, (g-H_2O)/(g-K_2CO_3/V)
a_c	equilibrium water uptake under particular conditions, (g-H_2O)/(g-K_2CO_3/V)
m_0	mass of completely dry material, mg
m_{max}	maximal mass of water sorbed by the composite, mg
M_{H2O}	molar mass of H_2O, g/mol
M_{K2CO3}	molar mass of K_2CO_3, g/mol
$\Delta_r H^o_{298}$	standard reaction enthalpy at 298 K, kJ/mol
P(H_2O)	water vapor pressure for a current experiment, mbar
P_{eq}	equilibrium pressure at a certain T, mbar
T_e	evaporator temperature, °C
T_h	hydration temperature, °C
Q_{ab}	absorption heat, kJ/mol
Q_r	reaction heat, kJ/mol
Q_m	melting heat, kJ/mol
Q_Σ	total hydration heat, kJ/mol
$W_{\tau 1/2}$	average heat release power over half-conversion period, W/kg
W_r	average heat storage or release power in a reactor, W/kg

Greek symbols

α	conversion
ω	weight content of the salt, %
$\tau_{1/2}$	half-conversion time, s
ρ_{com}	composite density, kg/m^3
ρ_{K2CO3}	K_2CO_3 density, kg/m^3

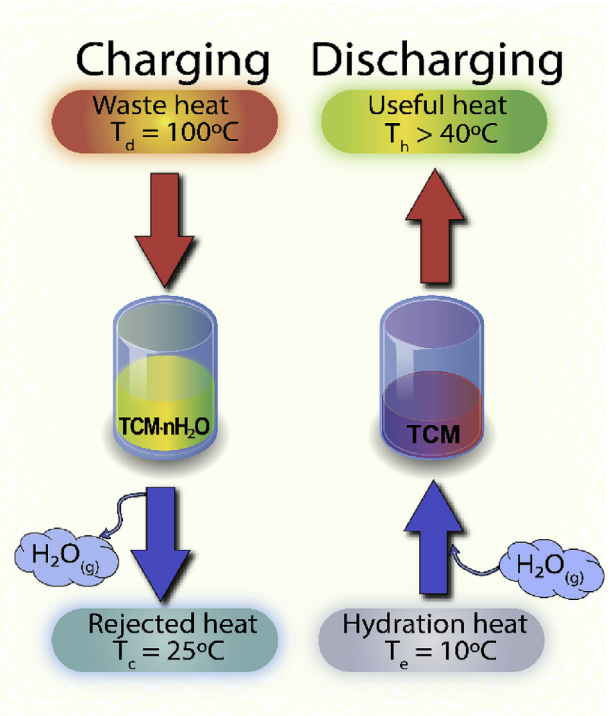

Fig. 1. Charging and discharging conditions of a TCES system for space heating/hot tap water production.

and does not degrade chemically. Both dehydration and hydration show good reversibility. The maximal heat storage density is 1.3 GJ/m^3 in an open system [11]. All these features render potassium carbonate a promising candidate for domestic heat storage applications.

Despite the advantages, application of K_2CO_3 for TCES is challenged by slow hydration rate, swelling/shrinking and particle agglomeration which eventually aggravates material performance in real devices. A possible approach to overcome these drawbacks is the use of porous matrices. The composites consisting of an active component (i.e. a salt) and a matrix that fully accommodates the active component were actively studied during the last decade [13]. The popular matrices are commercially produced adsorbents such as porous silica [14], alumina [15], zeolites [16], carbon-based materials [17] and some metal-organic frameworks [18]. Recently, siloxane polymer foams [19] and encapsulation of salt in methylcellulose shells were proposed for stabilization of some salts for the applications [20]. Besides preventing agglomeration of the salt particles, the matrices are often able to accommodate salt solution inside pores which expands their range of operational conditions.

Vermiculite is an alumosilicate clay $(Mg,Fe^{+2},Fe^{+3})_3[(Al,Si)_4O_{10}](OH)_2 \cdot 4H_2O$ which can be rapidly expanded by thermal treatment forming a porous structure with slit-shaped pores of several micrometers in size [21]. Due to high pore volume, this material was recently identified as a promising host matrix for accommodation of PCMs [22] and some thermochemical materials such as LiCl [23], $LiNO_3$ [24], $BaCl_2$ [25] and metal hydroxides [26,27]. Due to the high porosity of the matrix (~0.8) typical values of heat storage densities for such materials are relatively high as compared to other composites salt/matrix. They vary from 0.3 GJ/m^3 (83 kWh/m^3) for $CaCl_2$-based composites [24] to 0.9 GJ/m^3 (250 kWh/m^3) for LiCl-based composites [28] per 1 cubic meter of a bed and depend on the hydration conditions suitable for a particular heating or cooling application. The lower the heat release temperature and/or higher evaporation temperature the more heat can be released in the course of hydration due to absorption of the water vapor by the salt solution in pores. While it is a common opinion that these composites are promising for applications in thermochemical systems, there is no proof of cyclic stability of such composites in the literature and the state of a confined salt after hydration/dehydration cycling is poorly studied.

This work addresses the stability of the novel composite "K_2CO_3 in expanded vermiculite" with respect to hydration/dehydration

Please cite this article as: A.I. Shkatulov et al., Stabilization of K_2CO_3 in vermiculite for thermochemical energy storage, Renewable Energy, https://doi.org/10.1016/j.renene.2019.11.119

cycling and deliquescence with the emphasis made on material state. The goal of the work is a comprehensive study of the composite cyclic stability: 1) chemical stability; 2) changes in morphology and porosity of the composite grains; 3) grain size evolution and stability of the bed before and after cycling in a lab-scale bed reactor. Moreover, hydration/dehydration kinetics, water sorption isotherms, and conversion stability in the cycles with the salt deliquescence are reported, heat storage density is evaluated and application of the new composite for space heating is discussed.

2. Experimental

2.1. Material preparation

The composite K_2CO_3 in pores of expanded vermiculite, hereinafter referred to as K_2CO_3/V, was prepared by impregnation of K_2CO_3 solution into the vermiculite pores. The expanded vermiculite (Sigma Aldrich, CAS #1318-00-9) was sieved (grain size 1-2 mm) and dried overnight at 160 °C. After that, a saturated at room temperature K_2CO_3 solution (53 wt%) was added to the vermiculite grains (2.8 ml of solution per 1 g of vermiculite). The impregnated material (~50 g) was then dried by using a rotary evaporator, under vacuum and intense rotation at 75 °C to ensure uniform impregnation. In order to dehydrate the material completely, the further drying was carried out at 160 °C overnight, which also removed possible $KHCO_3$ impurities. The weight content of K_2CO_3 in the dry composite determined by weighing of the K_2CO_3/V batch was 69%.

The dry K_2CO_3/V was cycled in a setup imitating a closed thermochemical system (Fig. 2). A portion of K_2CO_3/V (~20 g, 50 cm^3) with grain size 1-2 mm was loaded into a bed reactor equipped with a heater. The system was vacuumed with the reactor being maintained at 120 °C to ensure complete drying of the material before the experiment. After that, the vacuum pump was disconnected and the water vapor was introduced to the reactor by connecting the reactor to the evaporator/condenser with liquid water at a constant temperature T_e = 19 °C. This temperature was maintained constant during the experiment by the thermostat. Then the temperature of the reactor was set to 40 °C for 9 h in order to perform the hydration. The cycling was carried out by means of temperature swinging from 40 °C (hydration, 9 h) to 120 °C (dehydration, 3 h) and backwards while maintaining T_e = 19 °C (this corresponds to $P(H_2O)$ = 23 mbar). After 12, 23 and 54 cycles, part of the material (100-150 mg) was picked from the bed in dehydrated form for characterization. The cycled composites will be referred to as K_2CO_3/V-X where X is the number of cycles. In total, 74 hydration-dehydration cycles were carried out.

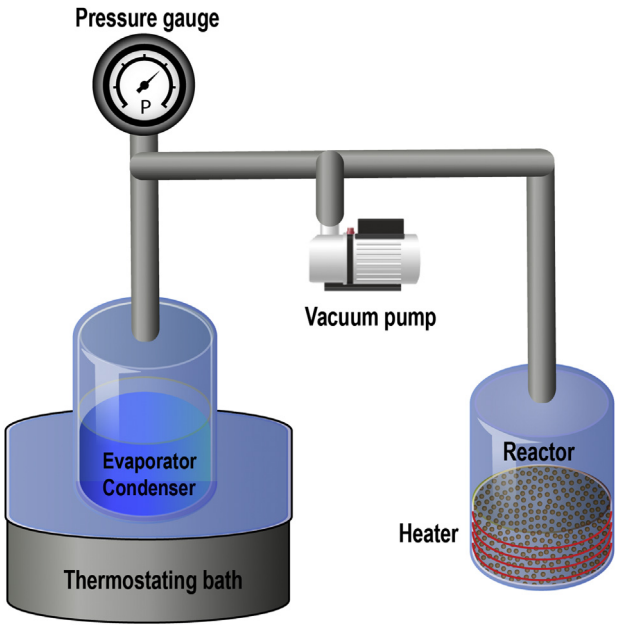

Fig. 2. A scheme of the setup for cycling of the K_2CO_3/V composite.

2.2. Material characterization

The as-prepared and cycled composites were characterized by a series of methods investigating stability, reaction kinetics and salt state in the course of the cycling.

Scanning electron microscopy (SEM) was carried out by using the electron microscope FEI Quanta 600. Dry composite grains were placed on an aluminum stage covered with double-side gluing carbon tape. The microscope chamber was vacuumed down to $3 \cdot 10^{-5}$ mbar and electron beam with accelerating voltage of 20 kV was used to obtain the SEM images. Energy-dispersive X-ray spectroscopy (EDS) mapping was carried out with the resolution of 124 eV in the range 0–8 keV. Silicon and potassium spectral bands were used to distinguish between the K_2CO_3 and vermiculite which contains mainly Si and O [29].

X-Ray diffraction (XRD) analysis was carried out by using Rigaku Miniflex 600 benchtop X-Ray diffractometer (θ-2θ geometry). The scanning was performed in air, in the 2θ range of 5-60°, with the scanning step of 0.02° and 1 s accumulation time. Prior to the measurements the dry samples were powdered by means of a Fritsch pulverisette 5 ball grinder (agate balls, 200 rpm, 30 min). The software Rigaku PDXL2 was used to analyze the XRD data.

Grain size distribution was determined by photographing the composite grains (with a scale ruler) on a black background using a digital camera (Canon EOS 700D, 15 MP) on a stand (KAISER RS 2 CP) followed by images processing by means of MATLAB. An ellipsoid was drawn around each composite particle and length of the shorter axis was taken as particle size since this parameter ensures passing a grain through the sieves used to separate fractions. About 800 grains of K_2CO_3/V and K_2CO_3/V-74 were photographed in order to investigate the size distribution.

Thermogravimetric analysis (TGA) was used to study hydration and dehydration kinetics by means of a Mettler Toledo© TGA/SDTA 851e thermobalance equipped with a humidifier and flow controllers which created and maintained a water vapor pressure of 14 mbar in the flow of N_2 (Fig. 3). The relative humidity inside the chamber was calibrated by using deliquescence points of inorganic salts (LiCl, $MgCl_2$, K_2CO_3, CH_3COOK). The temperature was verified by using the melting point of indium.

Vermiculite is a matrix with large pores of several micrometers and very low physical adsorption values due to low specific surface area (typical values are 2–3 m^3/g). Therefore, no size effects are observed for the salt in such composites (in other words, the phase diagram in Fig. 3 does not change) and adsorption of H_2O on the matrix surface can be neglected. This makes possible application of "traditional" kinetic analysis for the K_2CO_3 confined in vermiculite pores.

The hydration kinetics experiments were performed at various temperatures (30–48 °C) and water vapor pressure of 14 mbar in air flow (300 ml/min). Prior to hydration the loaded samples were fully dehydrated at T = 160 °C in dry flow to determine the dry mass m_0. Then the water vapor was introduced and hydration kinetic curves were measured.

Dehydration kinetics experiments were conducted at the same pressure and higher temperatures of 75, 85 and 95 °C (Fig. 3). Before dehydration, the material was saturated by placing a dry

Please cite this article as: A.I. Shkatulov et al., Stabilization of K_2CO_3 in vermiculite for thermochemical energy storage, Renewable Energy, https://doi.org/10.1016/j.renene.2019.11.119

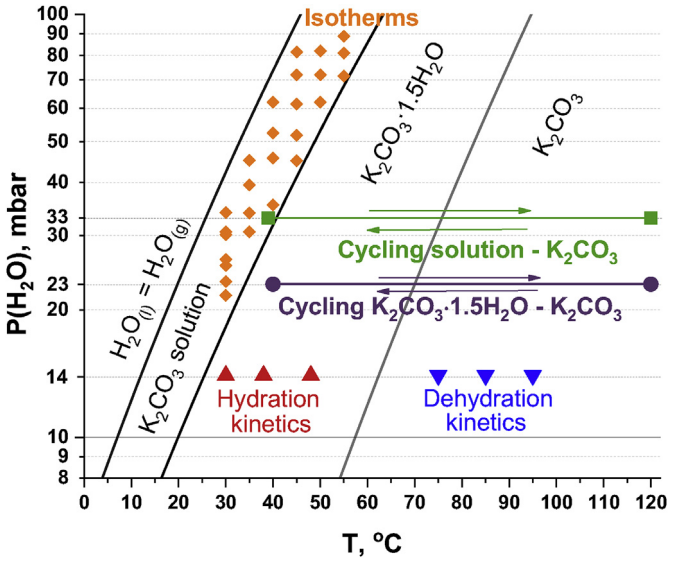

Fig. 3. Conditions of kinetic TGA, equilibrium DVS and cycling experiments plotted on a phase diagram of K_2CO_3–H_2O system. The conditions are marked as (●) for cycling $K_2CO_3 \cdot 1.5H_2O$ – K_2CO_3, (■) for cycling solution – K_2CO_3, (▲) – for hydration kinetics measurements, (▼) – for dehydration kinetics measurement, (♦) – for absorption isotherms of K_2CO_3 solution in vermiculite.

K_2CO_3/V sample in a desiccator at the fixed relative humidity of 33% (T = 25 °C) over saturated $MgCl_2$ solution overnight. The completeness of hydration was confirmed by weight loss during the drying at 160 °C which followed every experiment. For all the experiments the initial sample contained 1.48–1.49 molecules of water per one K_2CO_3 formula unit. A pan with the hydrated sample was quickly (~1 min) inserted to the pre-heated measurement cell which was then immediately closed.

Mass change in the course of all TG experiments and mass content of K_2CO_3 in the composite, ω, were used to determine the conversion, α, of K_2CO_3 to the sesquihydrate ($K_2CO_3 \cdot 1.5H_2O$) as follows:

$$\alpha = \frac{m(t) - m_0}{m_{max}}, \quad (2)$$

where $m(t)$ is mass at the moment t, m_{max} is maximal mass of water sorbed by the composite calculated based on reaction (1) stoichiometry and mass content of K_2CO_3 in the material:

$$m_{max} = 1.5 m_0 \omega \frac{M_{H_2O}}{M_{K_2CO_3}}, \quad (3)$$

where M_{H_2O} and $M_{K_2CO_3}$ are molar masses of water ant K_2CO_3, respectively.

Another cycling experiment verifying the material stability under the K_2CO_3 deliquescence conditions (hereinafter referred to DC-cycling) was carried out by using the setup with the bed reactor (Fig. 2) at evaporation temperature T_e = 25 °C (P(H_2O) = 32 mbar) in order to find whether the repetitive dissolution/recrystallization of the salt inside vermiculite pores affects the material performance. The chosen cycle duration (4 h of dehydration and 6 h of hydration) ensured the deliquescence of the salt and is considered as a compromise between the sorption value in the cycling experiment and overall experiment duration. For this experiment the reactor was put on a balance to register its weight change which was then normalized per 1 g of the composite.

Mercury intrusion porosimetry (MIP) was carried out by means of Micrometrics ASAP 2060 apparatus. A dehydrated dry material (around 100 mg) was loaded in an automatic porosimeter. A solid penetrometer (3 cm^3) with stem volume 0.412 cm^3 was used. The range of pressures used was 0.0007–227.5270 MPa). The mercury intrusion data was analyzed by means of AutoPore IV 9500 software.

Dynamic vapor sorption (DVS) was used to measure equilibrium water vapor absorption by the composites. The absorption isotherms were measured by using a TA Instruments® QS 5000 SA thermobalance at T = 30–55 °C and P(H_2O) = 22-117 mbar corresponding to deliquescence conditions of K_2CO_3 (Fig. 3). The dry K_2CO_3/V (ca. 12 mg) was loaded into a reaction chamber purged with N_2 which was then stabilized at a constant temperature. Water vapor was introduced into a stream of pure (>99.999%) nitrogen (ca. 500 ml/min) to create a certain water vapor pressure over the sample and weight change was registered. After equilibrium was reached, the RH was raised in a stepwise manner at a constant temperature. Every isotherm was measured for a new specimen of dry K_2CO_3/V.

3. Results and discussion

3.1. X-ray diffraction (XRD) analysis

Potassium carbonate could react with alumosilicate matrices such as vermiculite forming silicates in the course of the cycling which would make the composite chemically unstable. In order to verify the chemical stability of the composite with respect to this process, the powder X-Ray diffraction analysis was performed. The powder XRD pattern of the cycled composite K_2CO_3/V-74 exhibits only reflexes of K_2CO_3, $K_2CO_3 \cdot 1.5H_2O$ (due to some exposure to the ambient moisture) and vermiculite phases. The vermiculite reflexes were identified by XRD analysis of the pure matrix and their positions correspond to the ones in the K_2CO_3/V-74 (Fig. 4). It is noteworthy that no traces of potassium silicates are found. Moreover, the initial and cycled composites exhibit similar positions of the reflexes for all the phases. Thus, the XRD analysis showed that under the cycling conditions the composite K_2CO_3/V-74 consists of potassium carbonate and vermiculite which do not chemically interact with each other for at least 74 hydration/dehydration

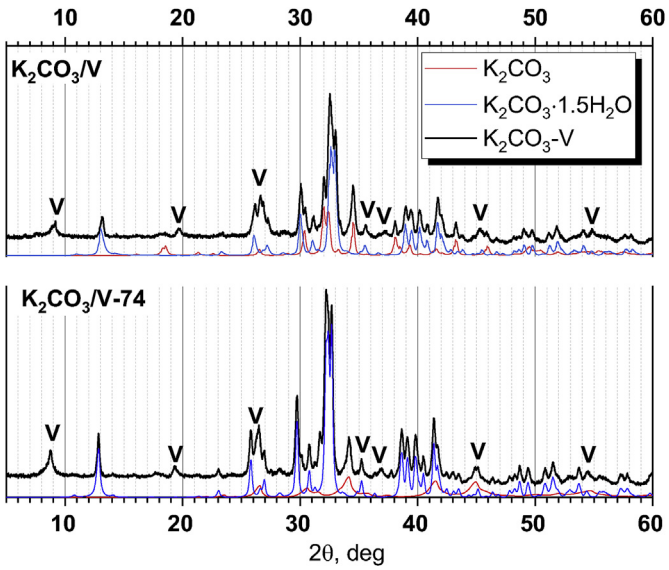

Fig. 4. Measured (black) and calculated (blue, red) XRD profiles of K2CO3/V, K2CO3/V-74. V stands for vermiculite reflexes. (For interpretation of the references to colour in this figure legend, the reader is referred to the Web version of this article.)

Please cite this article as: A.I. Shkatulov et al., Stabilization of K_2CO_3 in vermiculite for thermochemical energy storage, Renewable Energy, https://doi.org/10.1016/j.renene.2019.11.119

cycles.

3.2. Scanning electron microscopy (SEM)

Expanded vermiculite is a clay composed of alumosilicate layers that detach from each other in the course of thermal swelling [21]. The layered structure of expanded vermiculite conserves in the composite K_2CO_3/V. In Fig. 5a one can see the lamellas of vermiculite with irregular inclusions between them that can be ascribed to particles of the salt crystallized rapidly during the drying. Such a composite structure was confirmed by EDS mapping. In Fig. 5b, the K_2CO_3 (cyan) covers the vermiculite lamellas (magenta) and also fills the space between them. Large gaps between the layers which are not filled with the salt can be observed in a lower-magnification image (Fig. 5a).

After twelve hydration-dehydration cycles, the appearance of the salt dramatically changes from irregularly-shaped particles to agglomerates of 2–3 μm crystallites with crystal habits clearly visible in some cases (red circles on Fig. 6a). This self-dispersion of K_2CO_3 after several cycles may be attributed to cracking of the salt hydrate typically occurring due to mechanical stresses [30] followed by recrystallization of smaller $K_2CO_3 \cdot 1.5H_2O$ particles during hydration.

Further cycling leads to further filling of the gaps between vermiculite sheets (blue in Fig. 6b) by the salt particles (red in Fig. 6b). The self-dispersed K_2CO_3 forms its own porous structure which in the course of the cycling occupies the large gaps initially present between vermiculite layers (Fig. 6c and d). While salt particles change their morphology, the vermiculite conserves its layered structure which is not disintegrated and remains stable in the course of the cycling.

3.3. Mercury intrusion porosimetry (MIP)

According to the results of MIP, the pure expanded vermiculite possesses high porosity of 80% (Table 1) and pore volume of 3 cm^3/g (Fig. 7a) with around 90% of the pore volume belonging to the pores of less than 7 μm size (Fig. 7b).

The total pore volume normalized per 1 g of the matrix is 2.9 cm^3/g-V which suggests that the salt is not rigidly attached to the matrix lamellas and at maximal pressure (227.5 MPa) the mercury forces the salt removal to fill in the pores of the vermiculite matrix which appears to be mechanically stable judging from the proximity of the normalized pore volumes for vermiculite and K_2CO_3/V (Table 1). The normalized pore volume increases by 12% after 74 cycles suggesting that the vermiculite matrix slightly changes its porous structure (e.g. the interlamellar distance is increased) due to the mechanical forces exerting it in the course of the cycling. Alternatively, such increase may be explained by some loss of the salt from the pores of the matrix after the cycling.

3.4. Grain size stability

The stability of the bed was investigated by visual comparison and measuring the grain size of the composite. The visual appearance of K_2CO_3/V and K_2CO_3/V-74 is generally similar with some grains becoming larger after cycling (red circles of Fig. 8).

This result was corroborated by the analysis of grain size distribution. The majority of K_2CO_3/V grains are 1–2 mm in size with an average diameter of 1.6 mm (Fig. 9), which corresponds to the grain size of the vermiculite fraction taken for the composite preparation. The cycling broadens the size distribution as some grains larger than 2 mm are observed (some of them may be seen in Fig. 8). The average value of the grain size remains almost the same for K_2CO_3/V, K_2CO_3/V-12, K_2CO_3/V-23, K_2CO_3/V-54 and K_2CO_3/V-75 (inset graph on Fig. 9) thus evidencing stability of the material grain size. At the same time, the distribution becomes slightly broader suggesting that a minor part of grains agglomerates. This agglomeration may occur due to some K_2CO_3 on the external surface of the grains "gluing" them together. On the other hand, a minor part of the grains may decrease in size due to delamination.

Thus, the characterization of K_2CO_3/V and K_2CO_3/V-X by means of SEM and MIP has shown that the morphology of the grains changes dramatically due to salt self-dispersion. The porosity increases only slightly in the course of the cycling. Cycling in a lab-scale reactor showed that the average grain size remains constant with a broadening of particle size distribution.

3.5. Hydration/dehydration kinetics and heat storage density

Hydration of K_2CO_3 granules at $P(H_2O) = 14$ mbar (this corresponds to $T_e = 11$ °C) is a long-term process with the rate decreasing at higher temperatures since the system approaches to the equilibrium as oversaturation $P(H_2O)/P_{eq}$ drops from 10.9 to 2.7 (Fig. 10a). Dispersion of the K_2CO_3 in vermiculite considerably facilitates the hydration making half-conversion times 4-5 times shorter (Fig. 10b) for the same grain size. The phenomenon of increasing the hydration rate due to dispersion of a salt in a porous matrix was previously observed for many alike systems and can be attributed to the amelioration of transport in a composite grain

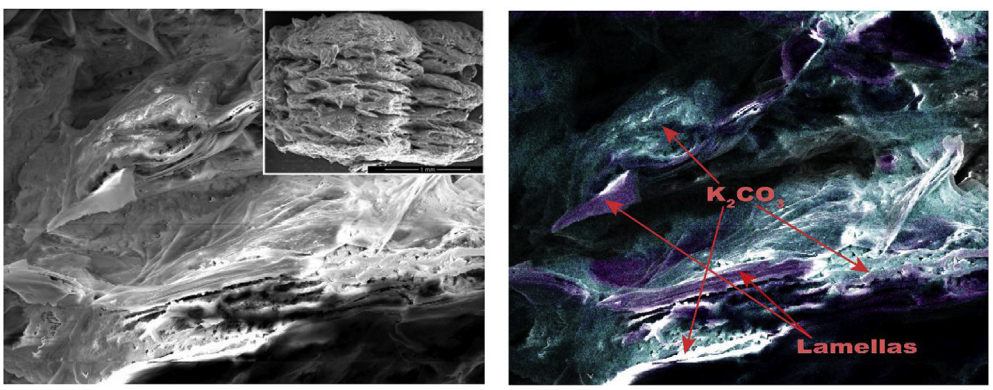

a b

Fig. 5. (a) A SEM image of K_2CO_3/V with (b) EDS mapping overlay (K – cyan, Si – magenta). (For interpretation of the references to colour in this figure legend, the reader is referred to the Web version of this article.)

Please cite this article as: A.I. Shkatulov et al., Stabilization of K_2CO_3 in vermiculite for thermochemical energy storage, Renewable Energy, https://doi.org/10.1016/j.renene.2019.11.119

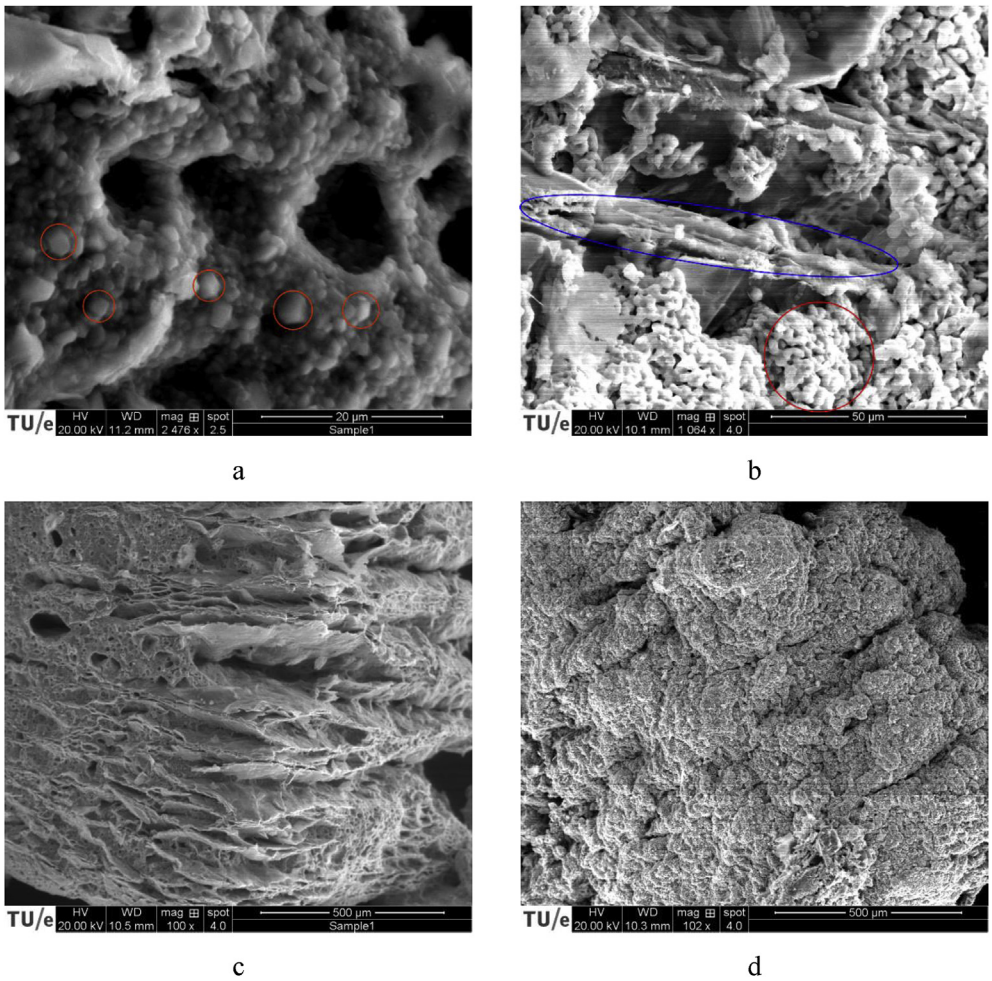

Fig. 6. SEM images of K_2CO_3/V-12 (a, c) and K_2CO_3/V-74 (b, d). Red circles represent salt crystallines, blue circles represent vermiculite lamellas. (For interpretation of the references to colour in this figure legend, the reader is referred to the Web version of this article.)

Table 1
Some characteristics of vermiculite and the composites determined by MIP.

Material	Pore volume, cm^3/g	Pore volume, cm^3/g-V	Porosity, %	Average pore size (4V/A),µm
Vermiculite	3.02	3.02	80.5	1.04
K_2CO_3/V	0.90	2.90	63.8	0.79
K_2CO_3/V-74	1.05	3.38	66.5	1.01

[13].

The half-conversion of K_2CO_3/V at 48 °C is reached after 1 h of hydration. This gives an average heat release power $W_{\tau 1/2} = 140$ W/kg as determined by Eq. (4):

$$W_{\tau_{1/2}} = \frac{1}{2} \cdot \frac{\omega \cdot \Delta_r H^o}{M_{K_2CO_3}} \cdot \frac{1}{\tau_{1/2}} \quad (4)$$

The dehydration of the $K_2CO_3 \cdot 1.5H_2O$ corresponds to charging of a thermal battery by external heat. This process goes slowly at T = 75 °C and P(H_2O) = 14 mbar with a pronounced induction period due to slow nuclei formation (Fig. 11). At the higher temperatures, the dehydration half-conversion is reached much faster (20 min at 95 °C) which may be considered practically promising. The composite K_2CO_3/V exhibits slightly shorter half-conversion times which suggests that dehydration is not sensitive neither to salt morphology nor to transport properties outside the K_2CO_3 particles and its rate is likely to be determined by local crystal transport phenomena such as transport of lattice defects or diffusion of water molecules to the external crystal surface, mechanical stresses and other local processes occurring in the course of dehydration of salt hydrates [30].

Hydration kinetics of the cycled K_2CO_3/V was studied at higher water vapor pressure P(H_2O) = 23 mbar to imitate conditions of the bed reactor cycling experiment (Fig. 3). Under these conditions, the reaction is faster and half-conversion of K_2CO_3/V hydration is reached already at 18 min with $W_{\tau_{1/2}=}$ 450 W/kg.

The cycling thus leads to the increase of initial hydration rate which remains almost constant for materials after 23 and 74 cycles (Fig. 12). A reason for such unusual behavior may be the self-dispersion of K_2CO_3 which creates additional porosity of the material and opens additional pathways for the water molecules.

The values of Volumetric heat Storage Density (VSD) for the composite were evaluated taking into account only reaction (1):

Please cite this article as: A.I. Shkatulov et al., Stabilization of K_2CO_3 in vermiculite for thermochemical energy storage, Renewable Energy, https://doi.org/10.1016/j.renene.2019.11.119

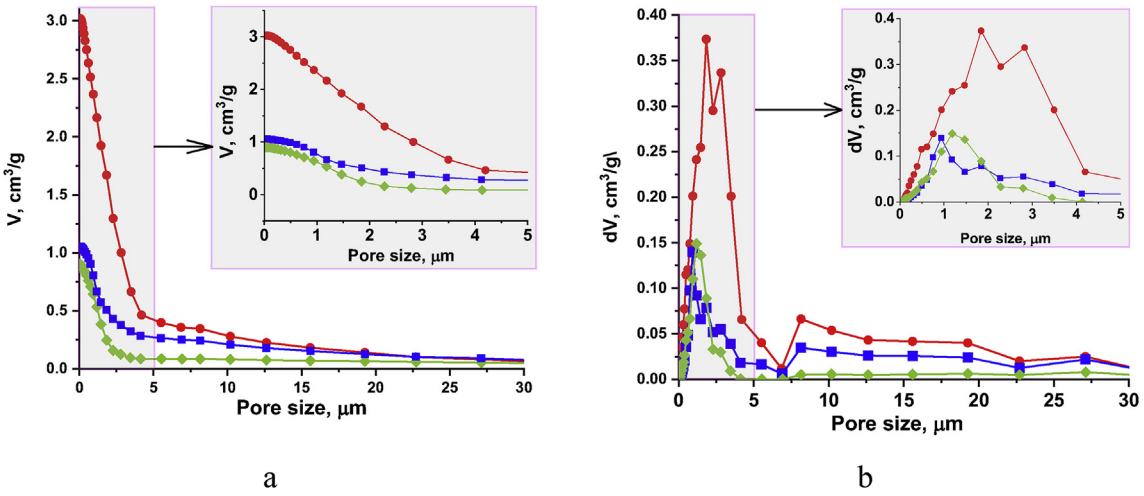

Fig. 7. Incremental (a) and cumulative (b) pore volume filled by mercury for vermiculite (●), K_2CO_3/V (♦) and K_2CO_3/V-74 (■).

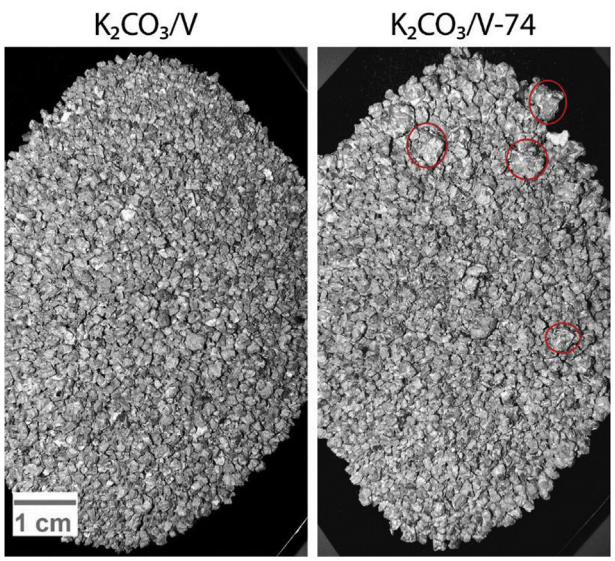

Fig. 8. Photographs of the K_2CO_3/V bed before cycling and after 74 hydration-dehydration cycles.

$$VSD_r = VSD_{K_2CO_3} \cdot \omega \cdot \frac{\rho_{com}}{\rho_{K_2CO_3}}, \quad (5)$$

where $VSD_{K_2CO_3}$ is maximal storage density for K_2CO_3 (1.3 GJ/m^3), ω is the mass content of K_2CO_3 in K_2CO_3/V (69 wt.%), ρ_{com} is composite density (kg/m^3) and ρK_2CO_3 is density of K_2CO_3 (2290 kg/m^3). The real density of the composite grains measured by mercury intrusion porosimetry (800 kg/m^3) was taken as ρ_{com} for the estimation of *VSD* on the grain level. According to the calculation, the matrix dilutes the active component lowering the *VSD* by a factor of 4 from 1.3 GJ/m^3 for bulk K_2CO_3 to 0.33 GJ/m^3 for K_2CO_3/V on the grain level.

For the bed, the value of ρ_{com} = 400 kg/m^3 corresponds to the measured density. The packing of K_2CO_3/V grains is thus very loose which further reduces the *VSD* by a factor of 2. The obtained values are comparable with *VSD* for phase-changing materials (PCMs) and PCM-based composites operating in the similar temperature region [24,31]. The VSD for such composites "Salt in a porous matrix" may be boosted up by using these materials under the salt deliquescence conditions which allows extraction of additional heat by exothermic water vapor absorption by the salt solution in pores.

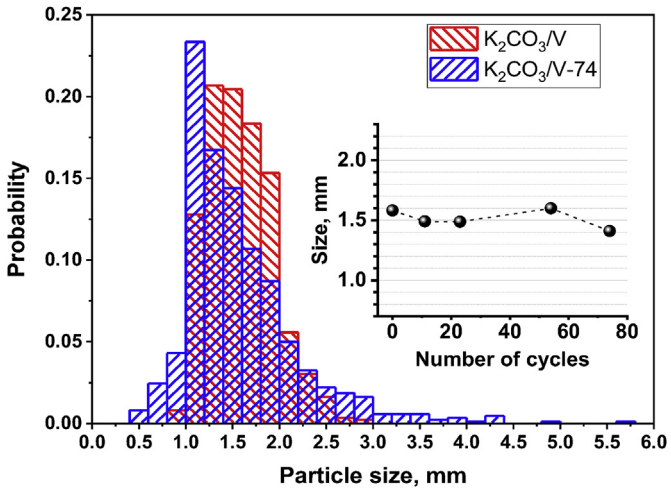

Fig. 9. Particle size distribution for K_2CO_3/V and K_2CO_3/V-74. The average particle size is shown by the inset graph.

3.6. Water absorption isotherms and heat storage density

The vermiculite matrix is known for its ability to retain solution due to capillary forces (the water uptake of the matrix itself is negligible). This effect may be used to extract more heat from the composite due to the absorption of water by the solution in pores. In order to make a quantitative estimation of this opportunity, the absorption isotherms were measured for the composite K_2CO_3/V. High values of water uptake *a* (g/g) can be achieved due to the high pore volume present in K_2CO_3/V.

The dependencies water uptake − P(H_2O) for a certain temperature are well fit by exponential law (Fig. 13a). The interpolated dependencies were used to build sorption isosteres (i.e. P-T dependencies for a fixed uptake *a*) which then were linearized in lnP − 1/RT coordinates in order to determine absorption heat from the slope of these lines. The dependency of isosteric heat on water uptake can be well described by the exponential law (Fig. 13b):

Please cite this article as: A.I. Shkatulov et al., Stabilization of K_2CO_3 in vermiculite for thermochemical energy storage, Renewable Energy, https://doi.org/10.1016/j.renene.2019.11.119

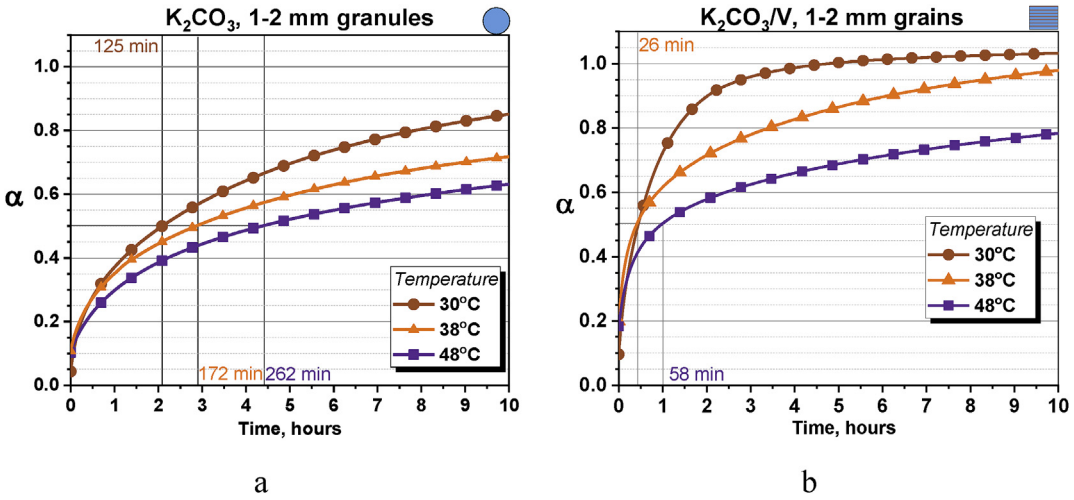

Fig. 10. Hydration kinetics at various temperatures for K_2CO_3 granules (a) in comparison with K_2CO_3/V grains (b) at water vapor pressure $P(H_2O)$ = 14 mbar and oversaturation $P(H_2O)/P_{eq}$ = 10.9 (T_h = 30 °C), 5.8 (38 °C) and 2.7 (48 °C).

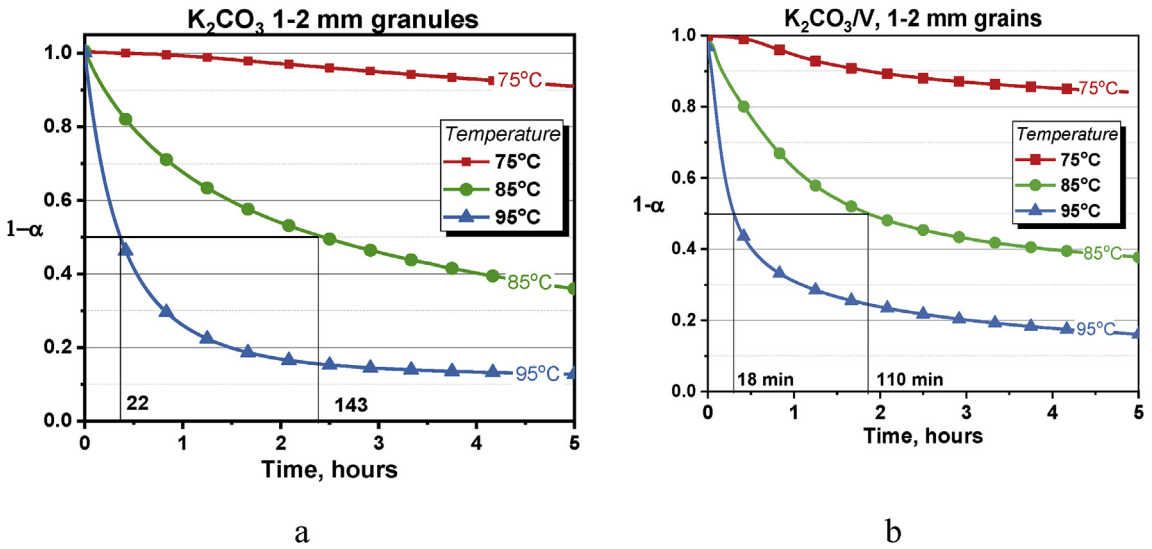

Fig. 11. Dehydration kinetics at various temperatures for K_2CO_3 granules (a) in comparison with K_2CO_3/V grains (b) at water vapor pressure $P(H_2O)$ = 14 mbar. $P(H_2O)/P_{eq}$ is 0.44 for T_h = 75 °C, 0.24 (85 °C) and 0.14 (95 °C).

$$Q_{ab} = 46171.75 + 67108.91e^{-\frac{a}{0.34132}}[J/mol]. \quad (6)$$

The hydration heat of K_2CO_3/V from anhydrous state to solution-in-pores state was evaluated by using the total hydration heat Q_Σ composed of three components, namely, hydration heat of K_2CO_3 according to reaction (1), Q_r, melting heat of $K_2CO_3 \cdot 1.5H_2O$ Q_m which was neglected and absorption heat evaluated using the uptake value a_c found from the absorption isotherms for a particular cycle with given T_e and T_h:

$$Q_\sum = Q_r + Q_m + Q_{abs}, Q_m \approx 0 \quad (7)$$

$$Q_r = \frac{\Delta_r H^o_{298}}{M_{K_2CO_3}} \omega \quad (8)$$

$$Q_{ab} = \int_{a_{0=0.135}}^{a_c} \frac{\overline{\Delta_{abs} H^o}(a)da}{M_{H_2O}} \quad (9)$$

The volumetric heat storage density under absorption conditions can then be evaluated as:

$$VSD_{ab} = Q_\sum \rho_{com} \quad (10)$$

According to Fig. 14, VSD on the bed level (assuming ρ_{com} = 400 kg/m^3) can reach values higher than 0.8 GJ/m^3 if one utilizes extra heat of deliquescence. Such values correspond to the state-of-the-art VSD for other composites salt/matrix [28,32]. The temperature lift of hydration (T_h - T_e) for the cycles with deliquescence is lower than for the case when only reaction (1) is used for the heat upgrade. In other words, the lower-grade heat is extracted if one uses deliquescence conditions. However, some promising cycles at T_h = 30–40 °C which may be used for space heating applications (e.g. warm floor) are marked by beads on

Please cite this article as: A.I. Shkatulov et al., Stabilization of K_2CO_3 in vermiculite for thermochemical energy storage, Renewable Energy, https://doi.org/10.1016/j.renene.2019.11.119

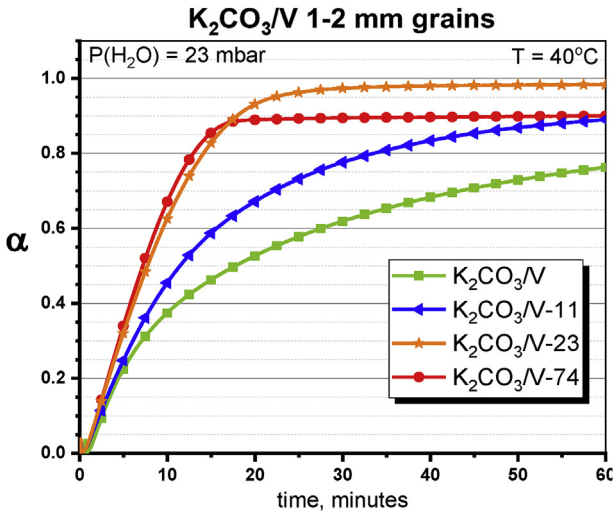

Fig. 12. Hydration kinetics of K_2CO_3/V and K_2CO_3/V-X (X = 11, 23, 74) at T = 40 °C and $P(H_2O)$ = 23 mbar. $P(H_2O)/P_{eq}$ = 8.1.

Fig. 14. Indeed, temperatures less than 25 °C are below a comfortable level while 30–40 °C heat may be used for space heating in some countries, for example, in "hot floor" systems. For a modern low-energy building in Europe (100 m^2) around 10-12 m^3 of the K_2CO_3/V composite should suffice the yearly need for space heating [28].

Thus, the volumetric heat storage density of K_2CO_3/V composite may be boosted up to 0.7–0.9 GJ/m^3 by extracting additional heat due to water absorption by K_2CO_3 solution in pores. The valuable heat may be extracted using lower-grade heat of 20–30 °C at hydration temperature T_h = 30–40 °C by which may be promising for space heating.

3.7. Cycling and charging/discharging power for cycles with deliquescence

Conversion stability of K_2CO_3/V was studied for a cycle with the salt deliquescence. For the study, a cycle with the highest temperature lift of 15 °C and maximal *VSD* of 0.71 GJ/m^3 (T_e = 25 °C, T_h = 40 °C) was chosen (red dot in Fig. 14).

The hydration/dehydration conversions, as well as the bed temperatures, are shown to be stable over at least 47 cycles (Fig. 15). The bed temperature was set to 40 °C, however, the real values were even higher thus showing discharge possibility at T_h = 43 °C.

Thus, cycling in a lab-scale reactor showed stable hydration and dehydration conversions over at least 47 cycles.

4. Conclusions

The composite K_2CO_3/expanded vermiculite for thermochemical energy storage (69 wt. % of K_2CO_3) was prepared by the dry impregnation method. Its chemical stability, morphological stability of the grains and grain size stability were experimentally studied.

The hydration kinetics of the composite K_2CO_3/V was studied by thermogravimetric analysis (TGA) at various temperatures (26–53 °C) and water vapor pressures (8-20 mbar). Dehydration kinetics was studied by TGA at T = 75–95 °C, $P(H_2O)$ = 12 mbar. Both processes were found to be 2-5 times faster for the composite in comparison with the appropriate mass of K_2CO_3 granules of the same size. Interestingly, cycling of the material made hydration rate faster, thus possibly indicating building up porosity upon cycling which was further confirmed by scanning electron microscopy.

The initial and cycled materials were characterized by scanning electron microscopy (SEM) with EDS mapping, X-Ray diffraction (XRD) analysis and mercury intrusion porosimetry (MIP). By means of MIP it was found that 90% of the salt fills the vermiculite pores with size less than 7 μm. After cycling the porosity increases by some 15% due to the pores larger than 7 μm. Morphology of the salt particles changes dramatically in the course of the cycling from irregular lumps of the K_2CO_3 to agglomerates of crystallites of 2–3 μm in size. The XRD analysis showed no chemical interaction of K_2CO_3 with vermiculite over at least 74 hydration/dehydration cycles.

The composite K_2CO_3/V can retain water solution of K_2CO_3 in the pores due co capillary forces. Water absorption isotherms of K_2CO_3 in vermiculite pores were obtained by means of dynamic vapor sorption (DVS) method. It was found that the composite can absorb 0.4–1.5 g/g of H_2O at 30–50 °C and water vapor pressures of 22–117 mbar. The volumetric heat storage density may thus be boosted up to 0.7–0.9 GJ/m^3 for conditions that may be promising for space heating. The material conversion was found to be stable over 47 such cycles with salt deliquescence.

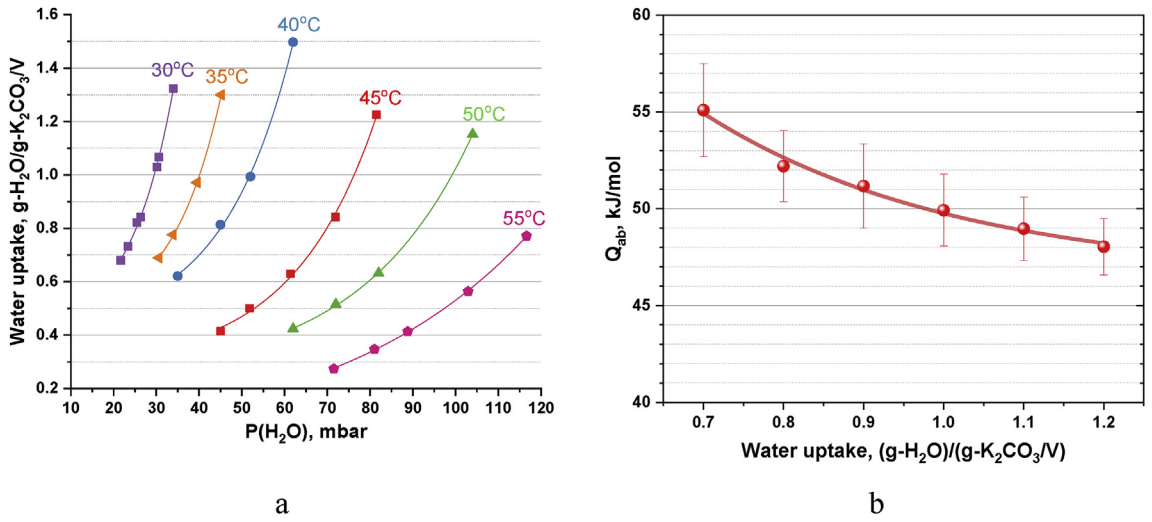

Fig. 13. Water sorption isotherms for K_2CO_3/V under the salt deliquescence conditions (a) and isosteric heat of absorption for different sorption values (b).

Please cite this article as: A.I. Shkatulov et al., Stabilization of K_2CO_3 in vermiculite for thermochemical energy storage, Renewable Energy, https://doi.org/10.1016/j.renene.2019.11.119

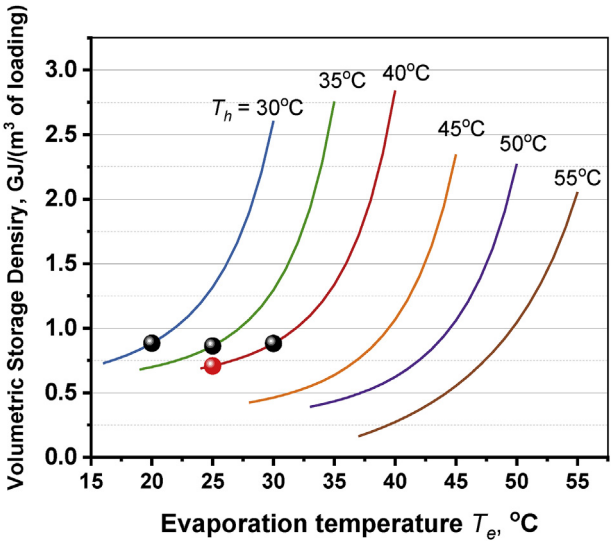

Fig. 14. Volumetric heat storage density by K_2CO_3/V composite ($\rho_{com} = 400$ kg/m^3) for various hydration temperatures T_h. The evaporation temperature T_e is restricted by the phase diagram from the lower side and by T_h from the upper one ($T_e < T_h$).

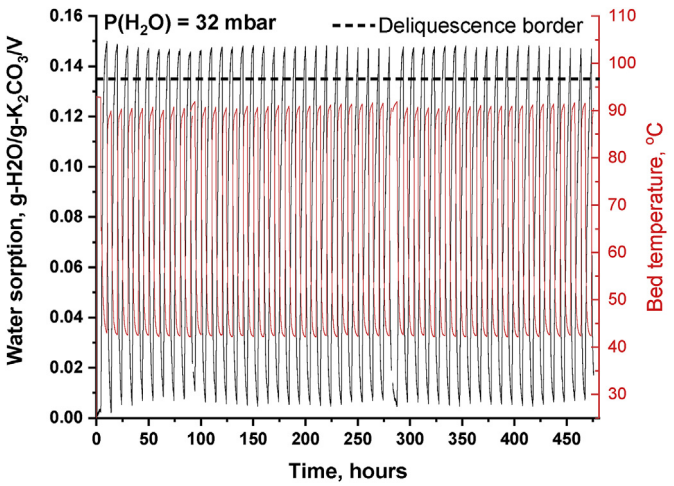

Fig. 15. Water sorption during cycling of K_2CO_3/V over 47 sorption/desorption cycles at $T_e = 25$ °C, $T_h = 40$ °C.

Thus, confinement of K_2CO_3 to the expanded vermiculite matrix was shown to ameliorate hydration and dehydration kinetics and stabilize the salt towards cycling. The composite retains solution in pores which expands the set of working conditions and allows for a boost of heat storage density through the advanced organization of a heat storage cycle. The composite may be promising for thermal energy storage.

Authors contribution

A.S. prepared the materials, conducted the experiments (except for MIP and EDS mapping) and wrote the manuscript, J.H. built the lab-scale setup used for the cycling, H.F. and H.H. actively took part in the experiment design and discussion of the results.

Declaration of competing interest

The authors declare no competing financial interest.

Acknowledgements

The authors are grateful to TKI Cap4Heat project for financial support. Special thanks are addressed to Peter Lipman for mercury intrusion porosimetry, Tijmen Vermeij for EDS mapping and Hans Dalderop for assistance with scanning electron microscopy.

References

[1] World Energy Outlook. https://www.iea.org/weo2018/, 2018. (Accessed 11 November 2019).
[2] F. Belaïd, Understanding the spectrum of domestic energy consumption: empirical evidence from France, Energy Policy 92 (2016) 220–233.
[3] Recent Advancements in Materials and Systems for Thermal Energy Storage, Springer Berlin Heidelberg, New York, NY, 2018.
[4] C. Prieto, P. Cooper, A.I. Fernández, L.F. Cabeza, Review of technology: thermochemical energy storage for concentrated solar power plants, Renew. Sustain. Energy Rev. 60 (2016) 909–929.
[5] W.E. Wentworth, E. Chen, Simple thermal decomposition reactions for storage of solar thermal energy, Sol. Energy 18 (1976) 205–214.
[6] K.E. N'Tsoukpoe, T. Schmidt, H.U. Rammelberg, B.A. Watts, W.K.L. Ruck, A systematic multi-step screening of numerous salt hydrates for low temperature thermochemical energy storage, Appl. Energy 124 (2014) 1–16.
[7] M. Deutsch, D. Müller, C. Aumeyr, C. Jordan, C. Gierl-Mayer, P. Weinberger, F. Winter, A. Werner, Systematic search algorithm for potential thermochemical energy storage systems, Appl. Energy 183 (2016) 113–120.
[8] P.A.J. Donkers, L.C. Sögütoglu, H.P. Huinink, H.R. Fischer, O.C.G. Adan, A review of salt hydrates for seasonal heat storage in domestic applications, Appl. Energy 199 (2017) 45–68.
[9] M. Richter, E.-M. Habermann, E. Siebecke, M. Linder, A systematic screening of salt hydrates as materials for a thermochemical heat transformer, Thermochim. Acta 659 (2018) 136–150.
[10] S. Kiyabu, J.S. Lowe, A. Ahmed, D.J. Siegel, Computational screening of hydration reactions for thermal energy storage: new materials and design rules, Chem. Mater. 30 (2018) 2006–2017.
[11] L.C. Sögütoglu, P.A.J. Donkers, H.R. Fischer, H.P. Huinink, O.C.G. Adan, In-depth investigation of thermochemical performance in a heat battery: cyclic analysis of K 2 CO 3 , MgCl 2 and Na 2 S, Appl. Energy 215 (2018) 159–173.
[12] L. Glasser, Thermodynamics of inorganic hydration and of humidity control, with an extensive database of salt hydrate Pairs, J. Chem. Eng. Data 59 (2014) 526–530.
[13] L.G. Gordeeva, Y.I. Aristov, Composites "salt inside porous matrix" for adsorption heat transformation: a current state-of-the-art and new trends, Int. J. Low Carbon Technol. 7 (2012) 288–302.
[14] M.M. Tokarev, L.G. Gordeeva, A.I. Shkatulov, Y.I. Aristov, Testing the lab-scale "Heat from Cold" prototype with the "LiCl/silica – methanol" working pair, Energy Convers. Manag. 159 (2018) 213–220.
[15] A. Jabbari-Hichri, S. Bennici, A. Auroux, Enhancing the heat storage density of silica–alumina by addition of hygroscopic salts (CaCl2 , Ba(OH)2 , and LiNO3), Sol. Energy Mater. Sol. Cells 140 (2015) 351–360.
[16] J.X. Xu, T.X. Li, J.W. Chao, T.S. Yan, R.Z. Wang, High energy-density multi-form thermochemical energy storage based on multi-step sorption processes, Energy 185 (2019) 1131–1142.
[17] L. Jiang, J. Gao, L. Wang, R. Wang, Y. Lu, A.P. Roskilly, Investigation on performance of multi-salt composite sorbents for multilevel sorption thermal energy storage, Appl. Energy 190 (2017) 1029–1038.
[18] A. Permyakova, K. Chang, J. Zhao, Z. Xie, H. Tang, B. Li, Z. Chang, Design of salt-metal organic frameworks composites for seasonal heat storage applications, J. Mater. Chem. A. 4 (2016) 51–58.
[19] V. Brancato, L. Calabrese, V. Palomba, A. Frazzica, M. Fullana-Puig, A. Solé, L.F. Cabeza, MgSO4·7H2O filled macro cellular foams: an innovative composite sorbent for thermo-chemical energy storage applications for solar buildings, Sol. Energy 173 (2018) 1278–1286.
[20] M. Gaeini, A.L. Rouws, J.W.O. Salari, H.A. Zondag, C.C.M. Rindt, Characterization of microencapsulated and impregnated porous host materials based on calcium chloride for thermochemical energy storage, Appl. Energy 212 (2018) 1165–1177.
[21] L.G. Gordeeva, E.N. Moroz, N.A. Rudina, Yul. Aristov, Formation of porous vermiculite structure in the course of swelling, Russ. J. Appl. Chem. 75 (2002) 357–361.
[22] P. Lv, C. Liu, Z. Rao, Review on clay mineral-based form-stable phase change materials: preparation, characterization and applications, Renew. Sustain. Energy Rev. 68 (2017) 707–726.
[23] Y. Zhang, R. Wang, T. Li, Y. Zhao, Thermochemical characterizations of novel vermiculite-LiCl composite sorbents for low-temperature heat storage, Energies 9 (2016) 854.
[24] R.J. Sutton, E. Jewell, J. Elvins, J.R. Searle, P. Jones, Characterising the discharge cycle of CaCl 2 and LiNO 3 hydrated salts within a vermiculite composite scaffold for thermochemical storage, Energy Build. 162 (2018) 109–120.
[25] J.V. Veselovskaya, R.E. Critoph, R.N. Thorpe, S. Metcalf, M.M. Tokarev, Yul. Aristov, Novel ammonia sorbents "porous matrix modified by active salt" for adsorptive heat transformation: 3. Testing of "BaCl2/vermiculite"

Please cite this article as: A.I. Shkatulov et al., Stabilization of K_2CO_3 in vermiculite for thermochemical energy storage, Renewable Energy, https://doi.org/10.1016/j.renene.2019.11.119

composite in a lab-scale adsorption chiller, Appl. Therm. Eng. 30 (2010) 1188–1192.
[26] A. Shkatulov, J. Ryu, Y. Kato, Y. Aristov, Composite material " Mg(OH)2/vermiculite": a promising new candidate for storage of middle temperature heat, Energy 44 (2012) 1028–1034.
[27] J. Kariya, J. Ryu, Y. Kato, Development of thermal storage material using vermiculite and calcium hydroxide, Appl. Therm. Eng. 94 (2016) 186–192.
[28] A.D. Grekova, L.G. Gordeeva, Y.I. Aristov, Composite "LiCl/vermiculite" as advanced water sorbent for thermal energy storage, Appl. Therm. Eng. 124 (2017) 1401–1408.
[29] R. Neumann, G.E.L. Costa, J.C. Gaspar, M. Palmieri, S.E. e Silva, The mineral phase quantification of vermiculite and interstratified clay minerals-containing ores by X-ray diffraction and Rietveld method after K cation exchange, Miner. Eng. 24 (2011) 1323–1334.
[30] S. Chizhik, A. Matvienko, A. Sidelnikov, Spatially-ordered nano-sized crystallites formed by dehydration-induced single crystal cracking of CuCl2·2(H2O), CrystEngComm 20 (2018) 6005–6017.
[31] E.M. Shchukina, M. Graham, Z. Zheng, D.G. Shchukin, Nanoencapsulation of phase change materials for advanced thermal energy storage systems, Chem. Soc. Rev. 47 (2018) 4156–4175.
[32] E. Courbon, P. D'Ans, A. Permyakova, O. Skrylnyk, N. Steunou, M. Degrez, M. Frère, Further improvement of the synthesis of silica gel and CaCl2 composites: enhancement of energy storage density and stability over cycles for solar heat storage coupled with space heating applications, Sol. Energy 157 (2017) 532–541.

Please cite this article as: A.I. Shkatulov et al., Stabilization of K_2CO_3 in vermiculite for thermochemical energy storage, Renewable Energy, https://doi.org/10.1016/j.renene.2019.11.119